Fibre Bragg Grating and No-Core Fibre in Variation of SRI

Siti Nur Aizatti Rohizad[a], Suzairi Daud[a,b], Esmafatinsyafiqa Multar[a], Nurul Shuhada Tan Halid[a] and Ahmad Fakhrurrazi Ahmad Noorden[c]

[a]Department of Physics, Faculty of Science, Universiti Teknologi Malaysia, 81310 Johor Bahru, Johor, Malaysia.

[b]Laser Center, Ibnu Sina Institute for Scientific & Industrial Research, Universiti Teknologi Malaysia, 81310 Johor Bahru, Johor, Malaysia.

[c]Department of Physics, Kulliyah of Science, International Islamic University Malaysia, Bandar Indera Mahkota, 25200 Kuantan, Pahang, Malaysia.

Abstract. In this work, Fibre Bragg Grating (FBG) and no-core fibre (NCF) sensors been investigated in different surrounding refractive index (SRI). FBG with 1550 nm wavelength attached with 5 cm length of NCF is used as SRI sensing probe. The sensitivity of the system was evaluated in different types of solutions which are ethylene glycol (18 % EG, 40 % EG, 60 % EG, 80 % EG, 100 % EG) and glycerol at room temperature. The dependence of the FBG and NCF wavelengths shift in spectral response versus different SRI has shown a linear relationship. The sensitivities of the system were 14.02 nm/RIU and 84.10 pm/RIU for FBG and NCF respectively.

Keywords: Fibre Bragg grating, no-core fibre, Bragg wavelength, surrounding refractive index, sensor

1. Introduction

Optical fibre has been used widely in communication system. However, it became popular in research area especially for sensing application due to their advantages such as electromagnetic immunity, allow monitoring with high multiplexing capacity, and reduce size and weight [1]. The diverse of sensing elements that has been explored including the measurement of temperature [2, 3, 4, 5], strain [6], displacement [7], pressure [8], surrounding refractive index (SRI) [9, 10] and curvature [11]. There are a few researches that have been done in SRI sensing by using single sensing elements or multiple sensing elements. As example, the application of SRI sensing by using Mach-Zehnder Interferometer (MZI) have been widely used for electromagnetic immunity, compact structures and high sensitivity [12] and LPFG is used for the device in optical communication [13]. However, the proposed system by MZI will cancel out when the silica thermo-optic coefficient present in the fibre sensor [1] while the LPFG can be affected by many kinds of perturbation [14].

In this work, the FBG-NCF based interferometer will be used for measurement of SRI. The wavelength of propagating light in FBG-NCF experienced consistent variation against the changes of SRI of the ambient material varies. The proposed solution provides a compact, ease of implementation system that able to sense SRI [2,15]. Moreover, it stands a great feasibility in both biology and chemical sensing applications.

2. Theory

NCF with a short length is joined between SMF and FBG by using fusion splicer. The multimode interference (MMI) is induced by the multiple modes that exhibited different longitudinal propagation. Eventually, the MMI formed the fourth self-image of input light in NCF. The lasing oscillation wavelength is related to MMI characteristic with equation:

$$\lambda_0 = 4\frac{n_{NCF}a_{NCF}^2}{L} \quad (1)$$

where L is the geometry length of the NCF, n_{NCF} is the refractive index of NCF, and a_{NCF}^2 is the diameter of NCF. A portion of light from NCF is propagated into FBG core between the splicing point of NCF and FBG, and others may propagate in cladding. Both of different path are experienced reflection at certain wavelength according to the design of FBG. Eventually, this will lead to the backward guided mode of the leading SMF. On the other hand, other modes that are not designed as reflective wavelength of FBG are propagated as core mode in SMF. These lights are then reflected at the edge of FBG-Air due to Fresnel reflection and propagated back to the SMF through NCF [16]. Due to the short length of FBG, the interference not able to induce large FSR, resulted relatively weak fringe visibility on the reflective spectra.

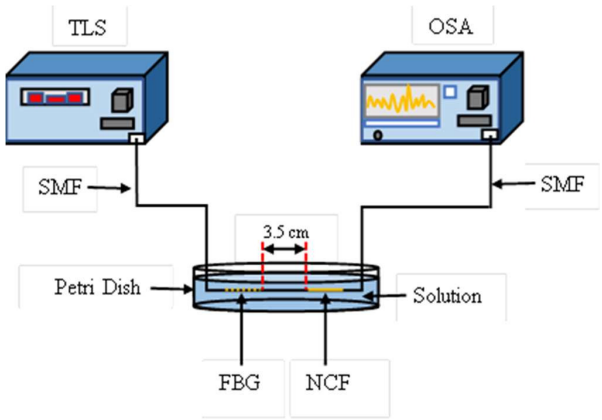

Figure 1: Setup of FBG-NCF sensor

3. Experimental set-up and discussion

The experimental set-up of this study is presented in Fig. 1, which consists of the proposed FBG-NCF sensor, a tunable laser source (TLS), and optical spectrum analyser (OSA). In the experiment, NCF with core diameter of 62.5 µm was used. It was exposed to the air at room temperature. The initial wavelength for each NCF with core diameter 62.5 µm is 1553.3520 nm. The FBG and NCF were joined with the distance of 3.5 cm as the optimum distance for FBG-NCF is between 3.0 cm to 3.5 cm. This is an experimentally optimized core diameter to achieve desired sensitivity. FBG-NCF sensor is soaked in the petri dish with different types of solutions; which are 18 % EG, 40 % EG, 60 %, 80 % EG, 100 % EG, and glycerol solutions at room temperature respectively. Fig. 2 shows the dependence of the NCF wavelengths shift in spectral response versus different SRI varying from 1.3503 RIU to 1.4635 RIU. Based on the graph plotted, the sensitivity of the FBG was calculated as 1.4167 nm/RIU via linear fitting method. When it was dipped in different solutions of ethanol glycol and glycerol solutions, the Bragg wavelength shift increase as it approaches the grating. From the observation, the FBG and NCF

wavelengths shifts towards the higher wavelength with increment of refractive index (RI) of the solutions.

The intensity of NCF in different solution was tested. Fig. 3 shows the relationship between power dip in variation solution with different RI. From the experiment done, the values of power dip increase as the RI increased and a very small deviation at RI of 1.3931 RIU can be observed. More fraction of the cladding mode becomes evanescent wave when RI approaches the SMF cladding RI. This caused an enhancement of the sensitivity. At 1.3931 RIU, NCF has a larger wavelength shift that leads to more power variation.

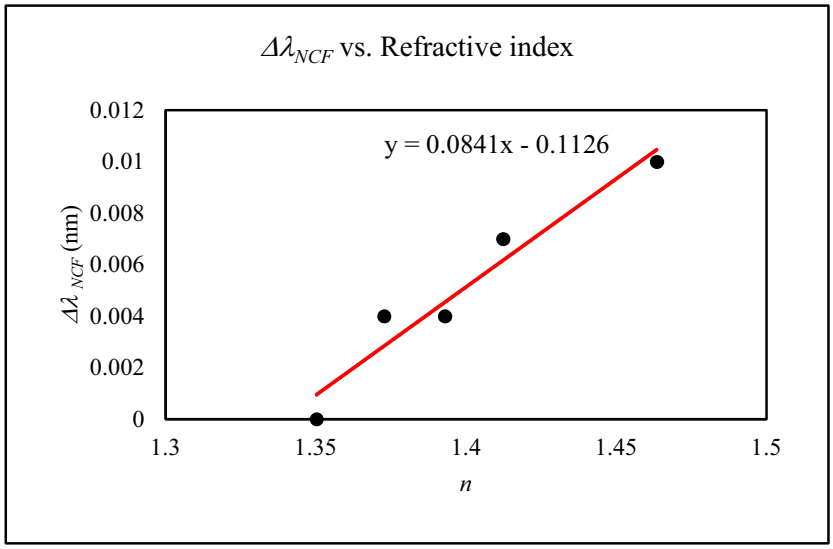

Figure 2: NCF wavelength shifts at different SRI

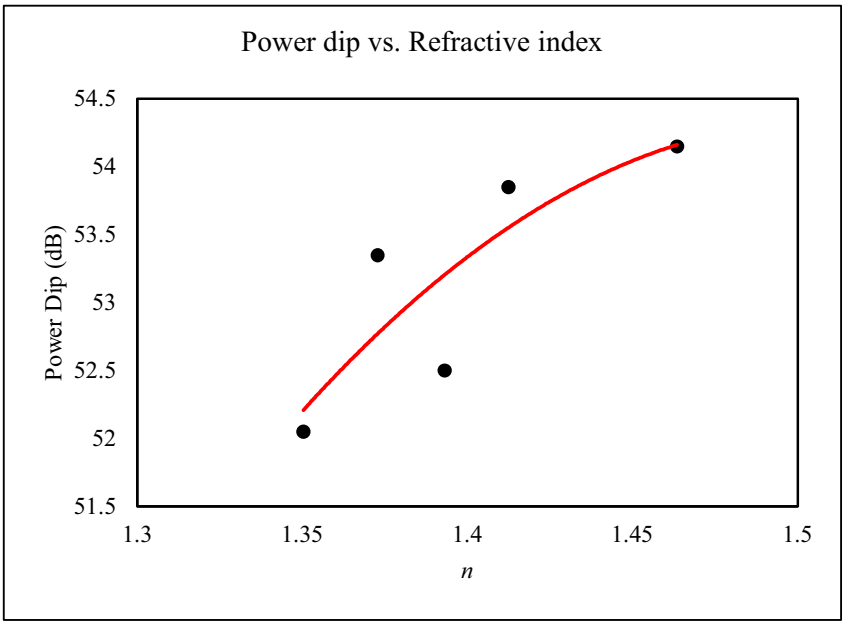

Figure 3: Power dip of NCF at different refractive index

Figure 4 shows the graph of Bragg and NCF wavelength shift versus RI of solutions at room temperature. From the graph plotted, it can be seen clearly that the overall trend of increment of FBG and NCF wavelength when RI is increased. The first peak shows the NCF sensing and FBG sensing is the other one. It can be seen a small shift of FBG spectra with increasing of SRI due to the reflected light.

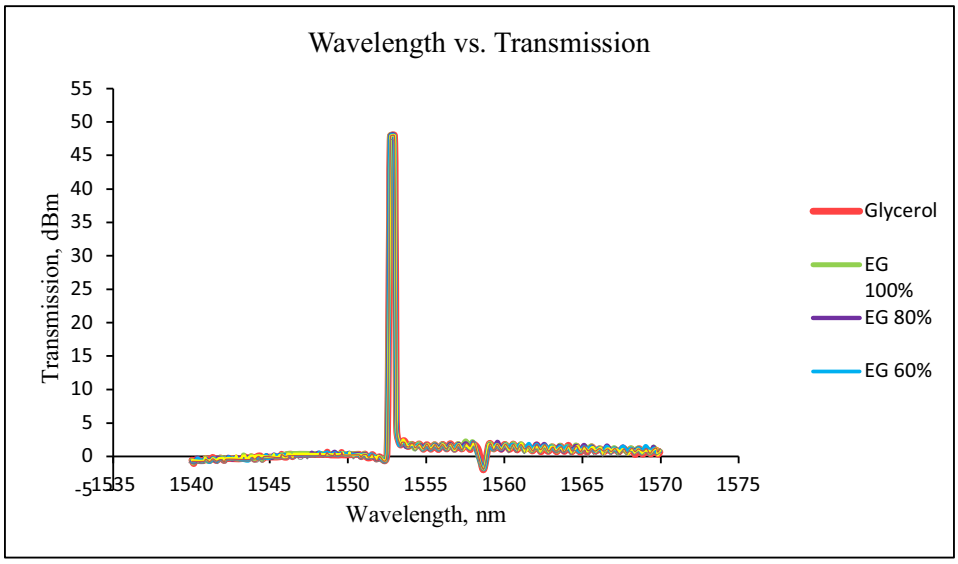

Figure 4: Graph of Bragg and NCF wavelength shift with different refractive index

Figure 5 shows the shift in wavelengths of FBG and NCF in air, 18 % EG, 40 % EG, 60 % EG, 80 % EG, 100 % EG and glycerol solutions respectively. As seen in Fig. 5, the sensitivity for FBG and NCF is calculated as 14.02 nm/RIU and 84.10 pm/RIU respectively via linear fitting method. The sensitivity determination depends on the loss-dip wavelength to be shifted.

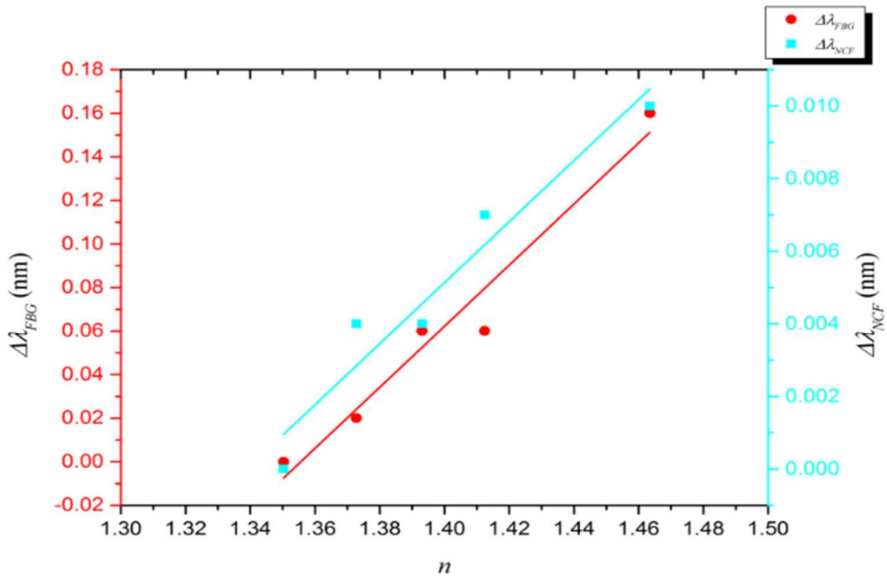

Figure 5: Wavelengths shift of FBG and NCF in different SRI

4. Conclusion

In this work, a novel and high feasibility interferometer that combined FBG and NCF were proposed and practically demonstrated for SRI sensing. The proposed design consists of an FBG and joined with a section of NCF that function as a multimode interferometer. The dependence of the NCF wavelengths shift in spectral response versus different SRI has shown a linear relationship.

Acknowledgement

Authors like to acknowledge Universiti Teknologi Malaysia for supporting this research via TDR grant vot. no. 07G29.

References

[1] Jin Y., Dong X., Gong H., and Shen C. 2009 *Microwave and Optical Technology Letters.* **52**.
[2] Daud S, Amiri IS, Noorden AFA, Ali J, Yupapin P. 2018 *Results in Physics 9*. 1685-1687.
[3] Zhang, C., Xu, S., Zhao, J., Li, H., Bai, H., & Miao, C. 2017 *Optical Engineering.* **56**.
Daud S, Abd Aziz, M. S., Chaudhary K T, Bahadoran, M., & Ali, J. 2016 *Jurnal Teknologi,* **78**.
[4] Daud S, Ahmad Noorden A F, Aziz M S, Chaudhary, K Bahadoran M, & Ali J. 2016 *Jurnal Teknologi,* **78**
[5] Bundalo, I., Nielsen, K., Woyessa, G., & Bang, O. 2017 *Optical Materials Express. 7* 967.
[6] Liu, W., Guo, Y., Xiong, L., & Kuang, Y. 2019*Sensor Review.* **39(**1), 87-98.
[7] Rosa, P., Thomas, S., Balakirev, F., Betts, J., Seo, S., Bauer, E., Jaime, M. *Sensors.* 2017 **17** 2543
[8] Zhang C., Xu S., Zhao J.,Li H., Bai H., and Miap C. 2017 *IEEE Photonics Journal*. **9**.

[9] Cięszczyk S., Kisała P., and Mroczka J., 1964 *Sensors.* 2019 **19**
[10] Osório, J. H., Oliveira, R., Aristilde, S., Chesini, G., Franco, M. A., Nogueira, R. N., & Cordeiro, C. M. *Optical Fiber Technology.* 2017 **34**, 86-90.
[11] Shao M., Qiao X., Fu H., Li H., Jia Z., and Zhou H. 2014 *IEEE Photonics Technology Letters* **26**.
[12] Chiang, K. S. *Asia Optical Fiber Communication and Optoelectronic Exposition and Conference* 2008.
[13] Miao Y., Liu B., Zhao Q. 2008 *International Conference on Advanced Infocomm Technology*.
[14] Lin G. R., Fu M. Y., Lee C. L., and Liu W. F. 2014 *Optical Engineering* **53**.
[15] Zhao, J., Wang, J., Zhang, C., Guo, C., Bai, H., Xu, W., Miao, C. 2016 *IEEE Photonics Journal* ***8*** 1-8.